

Three-Dimensional Location of the Main Immunogenic Region of the Acetylcholine Receptor

Rameen Beroukhim and Nigel Unwin

Medical Research Council Laboratory
of Molecular Biology
Cambridge, CB2 2QH
England

Summary

About two-thirds of the antibodies to the nicotinic acetylcholine (ACh) receptor in patients with the autoimmune disease myasthenia gravis bind to the main immunogenic region (MIR). This is a small, well-defined region on each of the two α subunits, containing residues 67–76 (α 67–76). By determining the structure of the ACh receptor complexed with two different fragments of an MIR-directed antibody, we have determined the three-dimensional location of the MIR (and therefore residues α 67–76) to be at the extreme synaptic end of each α subunit. The antibody fragments extend from the binding site away from the receptor axis and into the synaptic cleft, minimizing any steric interference neighboring ACh receptors might have with their binding.

Introduction

The muscular weakness and fatigue that characterize myasthenia gravis result from an antibody-mediated autoimmune response against the nicotinic acetylcholine (ACh) receptors of the neuromuscular junction (reviewed in Conti-Tronconi et al., 1994, Protti et al., 1993). Serum antibodies cross-link ACh receptors in the postsynaptic membrane and, by doing so, increase their degradation rate (Drachman et al., 1978; Pumplin and Drachman, 1983). Antibodies bound to ACh receptors may also activate the complement cascade (Tzartos et al., 1981). The result is a reduction in the number of receptors and an impairment of neuromuscular transmission.

The serum antibodies to the ACh receptor are heterogeneous, but about two-thirds of them bind to the main immunogenic region (MIR) (Tzartos et al., 1982), a small, well-defined region (Kordossi and Tzartos, 1989) on the extracellular part of the α subunit (Tzartos and Lindstrom, 1980). Antibodies to the MIR are pathologically significant; monoclonal antibodies (MAbs) to the MIR can, for instance, passively transfer experimental autoimmune myasthenia gravis in rats (Tzartos and Lindstrom, 1980).

Because the MIR plays an important role in myasthenia gravis, much effort has been directed toward characterizing the epitopes that compose it. These epitopes do not overlap with the ACh or bungarotoxin binding sites (Tzartos and Lindstrom, 1980; Tzartos et al., 1981). Many of the MIR-directed MAbs bind to the peptide corresponding to residues 67–76 of the α subunit. However, they bind more weakly to the peptide than to the native receptor; so, although the sequence α 67–76 forms a main constituent

loop of the MIR, other residues either form part of the MIR or stabilize its native conformation (Barkas et al., 1988; Tzartos et al., 1988). Peptide binding studies also indicate that the MIR may consist of overlapping epitopes for different MAbs (Tzartos et al., 1990). The species cross-reactivity of MAbs to the MIR shows it to be highly conserved among muscle-type ACh receptors (Tzartos et al., 1981); residues α 67–76 are also highly conserved among species (Bellone et al., 1989).

Most structural studies of the ACh receptor have used receptors derived from the electric organs of the electric ray *Torpedo*. These organs contain high densities of receptor dimers that are organized in partly crystalline arrays (Chang and Bock, 1977; Heuser and Salpeter, 1979). Under certain conditions after isolation (Brisson and Unwin, 1984; Kubalek et al., 1987), these dimers form ordered arrays on the surface of tubular vesicles, with their synaptic ends pointing outward. Electron crystallographic studies using flattened tubes preserved by either negative staining or rapid freezing show that the five subunits of the receptor are arranged in a pseudopentameric array around the central water-filled ion pathway (Brisson and Unwin, 1984; Brisson and Unwin, 1985; Mitra et al., 1989). The most detailed maps come from helical analyses of intact tubes that are rapidly frozen and then imaged by cryoelectron microscopy (Toyoshima and Unwin, 1988). Such analyses enable the averaging of information from the many receptors in the tubes while combining information from the different views available in a helix to obtain the three-dimensional structure. The subunits are 120 Å long rods that fit into a cylinder 80 Å in diameter and lie approximately perpendicular to the plane of the membrane. The ion pathway is narrow across the bilayer but widens outside it into a cylinder that is 20–25 Å in diameter and that extends 60–70 Å toward the synapse and 15–20 Å toward the interior of the cell. An extra mass is attached to the receptor at its intracellular end. This is probably the 43 kDa protein (Toyoshima and Unwin, 1988), which colocalizes with the receptor (Sealock et al., 1984) in approximately a 1:1 stoichiometry (LaRochelle and Froehner, 1986).

The location of the MIR in two dimensions was determined in a study that used electron microscopic images of tubes flattened in negative stain (Kubalek et al., 1987). Projection maps of various receptor–label complexes were produced; the label used to locate the MIR was a Fab fragment of MAb35 (see below). Fab35 appeared to attach to the outer edge of the receptor, at sites rotated approximately 36° relative to the α -bungarotoxin sites at the middle of the α subunits.

Although MAb35 was raised against ACh receptors from the electric eel, it cross-reacts with receptors from various sources (Tzartos et al., 1982). It binds strongly to the MIR on intact receptors (Tzartos et al., 1981), but does not bind significantly to peptides that correspond to residues α 67–76 (Tzartos et al., 1988). Mutagenesis studies on native receptors (Saedi et al., 1990) and further peptide binding

studies (Papadouli et al., 1993) show, however, that it does bind to some of those residues in native receptors (e.g., $\alpha 68$ and $\alpha 71$; Saedi et al., 1990). There is no indication that MAb35 directly interferes with receptor function (Lindstrom et al., 1981; Wan and Lindstrom, 1985), but it does cross-link ACh receptors in the postsynaptic membrane to increase their degradation rate (Conti-Tronconi et al., 1981; Tzartos et al., 1981). MAb35 can passively induce experimental autoimmune myasthenia gravis, as can $F(ab')_2 35$, a bivalent fragment of MAb35 that also cross-links receptors (Loutrari et al., 1992; Tzartos et al., 1987). Fab35, which protects receptors from being cross-linked by anti-MIR MAbs, can prevent 68% of the antigenic modulation caused by myasthenic patients' serum on muscle cells in culture (Tzartos et al., 1985).

The localization of the MIR in three dimensions and the architectural details of the attachment should provide important information about the interaction of pathologically significant antibodies with the ACh receptor. The localization of $\alpha 67-76$ in the receptor structure also places constraints on how the protein folds. We have determined the three-dimensional location of the MIR and the nature of antibody attachment by electron microscopy of ACh receptor tubes labeled with Fab35 or scFv35 (which contains only the variable domain of Fab35; Marks, 1992). The antibody fragments are found to bind to the extreme synaptic ends of the α subunits and to extend away from the receptor axis and toward the synaptic cleft.

Results

Preparations of ACh receptor-rich vesicles contain tubes of various diameters, each diameter corresponding to a different helical family and, therefore, a slightly different packing arrangement of the receptors (Toyoshima and Unwin, 1990). scFv35 and Fab35 were incubated with these tubes in suspension before being applied to electron microscope grids and examined by cryomethods (see Experimental Procedures). Images of 760 Å diameter tubes ((-16,6) helical family) and 750 Å diameter tubes ((-15,5) helical family) were analyzed to determine the structures of the scFv35- and Fab35-labeled receptors, respectively.

Figure 1 shows images of scFv35-labeled and Fab35-labeled tubes, together with unlabeled tubes of the same helical family as controls. The contrast in these images arises from the different densities of the protein (which appears dark) and the surrounding lipids and ice (which appear light). The synaptic ends of the closely packed receptors point outward (Brisson and Unwin, 1984), giving the edges of the tubes a striated appearance. The labeled tubes appear wider and more speckled than their unlabeled counterparts, owing to the presence of the antibody fragments.

The determination of the structures from the images was done by Fourier methods (see Experimental Procedures) to a resolution of 20 Å. The Fourier terms from three scFv35-labeled tubes and three Fab35-labeled tubes were averaged (see Experimental Procedures) to determine the respective structures. Previously determined structures of

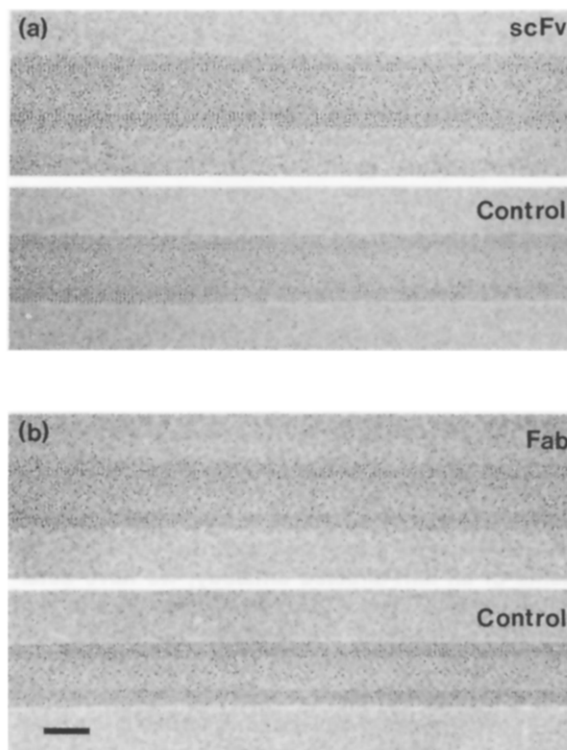


Figure 1. Images of Labeled and Unlabeled ACh Receptor Tubes Embedded in Ice

(a) scFv35-labeled and unlabeled (control) tubes of the same diameter (helical family (-16,6)) and (b) Fab35-labeled and control tubes of the same diameter (helical family (-15,5)). The synaptic ends of the closely packed receptors point outward, giving the edges of the tubes a striated appearance. The labeled tubes appear more speckled and slightly wider, owing to the binding of the antibody fragments. The (-16,6) tube that was labeled with scFv35 fragments has a slightly greater diameter than the (-15,5) tube that was labeled with Fab35 fragments. Bar, 500 Å.

the unlabeled receptors (Toyoshima and Unwin, 1990; Unwin, 1993) were used as controls. Details of the images and averaged datasets are summarized in Table 1.

Radial Density Distributions

Distributions of density against distance from the tube axes were calculated from the three-dimensional datasets (see Experimental Procedures) and are shown in Figure 2. The densities are lowest at radii of less than ~ 150 Å, at which they correspond to the ice that fills the tubes. They increase at higher radii ($\sim 150-400$ Å), owing to the presence of protein. At even higher radii (>400 Å), outside the tube, the densities decrease to the level of the ice. The density distributions of labeled and unlabeled (control) tubes are similar, except that the labeled tubes have extra shoulders of density (arrows) at high radii ($\sim 350-400$ Å). The shoulder is broader for the Fab35-labeled tubes than for the scFv35-labeled ones. These shoulders, which must be due to the antibody fragments, lie beyond the maximum radii of the unlabeled tubes, indicating that the antibody fragments attach to the end of the receptor. To determine

Table 1. Characteristics of Individual Images and Combined Datasets

	Number of Receptors	Phase Residual ^a	Weight in Final
scFv35			
Film number 4280	3560	23.5	0.18
Film number 4282	4360	24.2	0.23
Film number 4295	4820	16.1	0.59
Combined dataset	12,740	9.4	(1.0)
Control	8500	19.4	
Fab35			
Film number 4906	2430	26.2	0.33
Film number 5168	1700	28.6	0.33
Film number 5381	2180	26.3	0.33
Combined dataset	6310	19.9	(1.0)
Control	9420	15.6	

^a Amplitude-weighted phase residuals for 2-fold symmetry (difference from 0° or 180°).

the precise locations and architectural details of the antibody fragments, we next calculated and examined the three-dimensional maps.

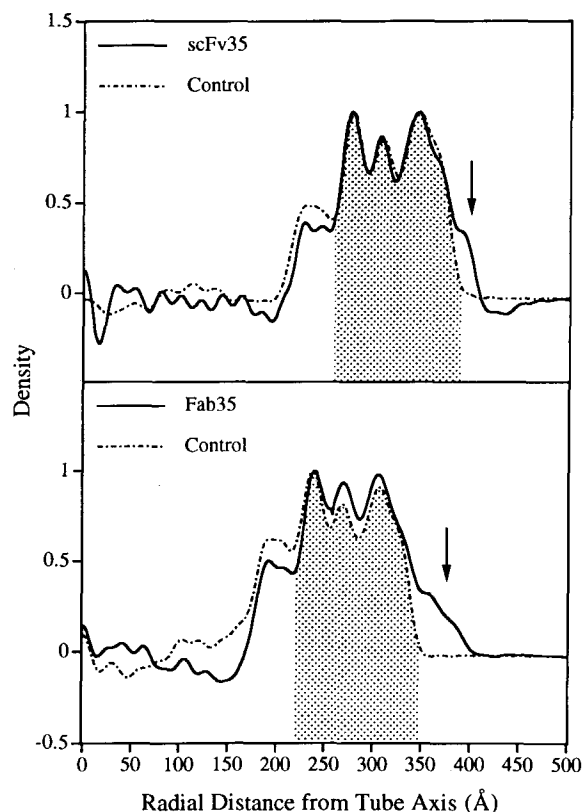


Figure 2. Locations of Antibody Fragments in Radial Plots

The graphs show how the density is distributed in labeled and unlabeled tubes as a function of radial distance from their axes. In both cases, the labeled tubes are compared with unlabeled tubes of the same diameter. The labeled tubes have extra shoulders of density at high radii (arrows). The shoulder on the Fab35-labeled density distribution is broader than the shoulder on the scFv35-labeled one because Fab fragments are larger than scFv fragments. The shaded region corresponds to the radial extent of the receptors; the differences in density at lower radii (below ~250 Å for the scFv-labeled tubes and ~225 Å for the Fab-labeled tubes) may reflect different amounts of bound cytoplasmic proteins, including the 43 kDa protein (LaRochelle and Froehner, 1986).

Antibody-Receptor Complexes

Figure 3 shows the structures of the scFv35-labeled and Fab35-labeled tubes in cross-section. The receptors project ~60–70 Å from the membrane surface, into the synaptic cleft. The antibody fragments (shaded grey) give rise to densities that are not present in corresponding maps of unlabeled receptors (Figure 3, Control). The Fab fragments (Figure 3, Fab) look similar to the scFv fragments (Figure 3, scFv), except that they present extra densities (marked as C in Figure 3, Fab) that extend further from the tube axis. These extra densities appear to correspond to the constant domains of the Fab fragments (see below).

Figure 4 shows the Fab35-labeled receptors in three dimensions. Maps that represent the densities in unlabeled tubes subtracted from those in corresponding labeled tubes show significant differences only in the region of the antibody fragments (data not shown), indicating that no major conformational change has occurred upon binding. The antibody fragments extend into the synaptic cleft (upward in our nomenclature) from protrusions (see also Figures 12 and 13 of Toyoshima and Unwin, 1990) at the ends of the α subunits. The regions thought to correspond to the constant domains of the Fab fragments (stippled red and marked as C) lie above the variable domains (marked as V), which are identified by their matching appearance to the scFv fragments (see below).

Antibody Fragments

Each antibody fragment mass connects equivalent α subunits (i.e., α_5 - α_5 and α_7 - α_7 ; see below) of neighboring receptors, giving the impression that the antibody fragments cross-link neighboring receptors. This is the case for both scFv35-labeled (Figure 5a) and Fab35-labeled (Figure 5b) receptors. Both types of antibody fragment are monovalent, however, so each mass should be composed of two fragments (V and C mark possible locations of variable and constant domains of individual antibody fragments; the constant domains are also stippled red), the densities having merged at this low resolution. The two sites on each receptor where the antibody fragments make contact are separated by about 144° around the central axis, which is the angle expected given that there is one subunit between the α subunits and the receptor has pseudo-5-fold symmetry.

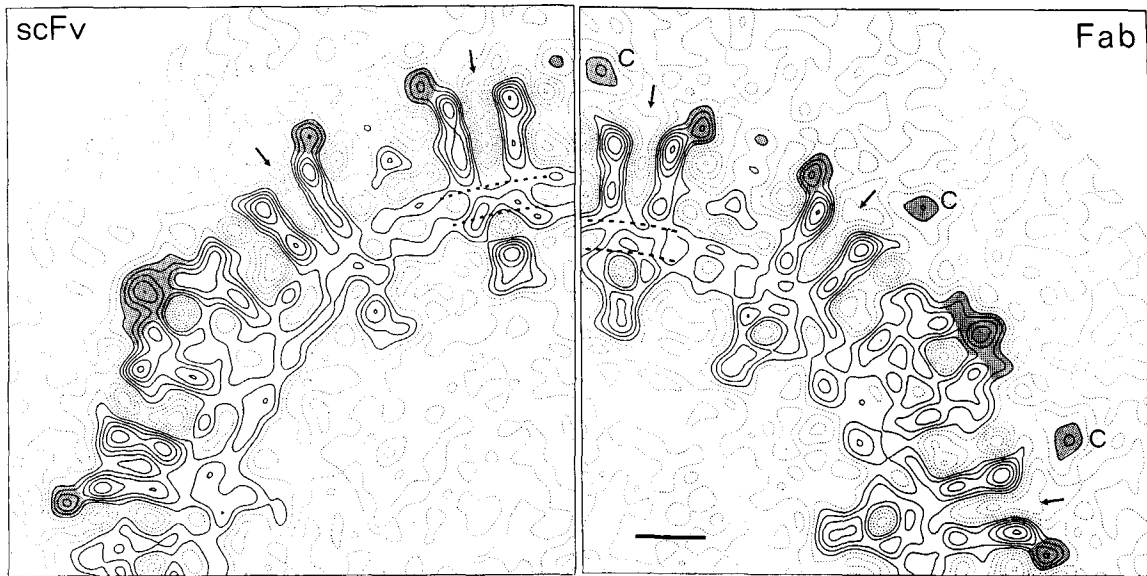


Figure 3. Antibody Fragments Attached to Receptors in Cross-Sections through the Tubes

Maps are from a scFv35-labeled tube (scFv35), a Fab35-labeled tube (Fab), and an unlabeled (Control) tube of the same diameter as in scFv. The antibody fragments (shaded grey) are at the synaptic ends of the receptors, which extend ~60–70 Å above the lipid bilayer (phospholipid head groups indicated by dashed lines). Additional density associated with the Fab fragments (marked as C) appears to correspond to their constant domains. The central ion pathways formed by the receptors are indicated by the arrows. The continuous contours indicate densities greater than that of water. Bar, 50 Å.

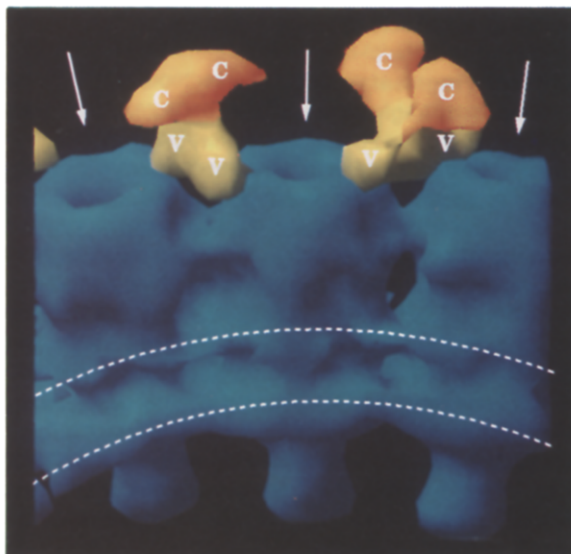


Figure 4. Side View of Fab Fragments Attached to the MIR of the Receptor

The Fab fragments (gold) are at the extreme synaptic end of the receptor (blue), attached to the rim surrounding the ion pathway (arrows). The constant domains (stippled red and marked as C) of those Fab fragments lie on top of the variable domains (marked as V) so the antibody fragments project from the binding site toward the synaptic cleft. The dashed lines denote the phospholipid head groups in the bilayer and are separated by about 40 Å.

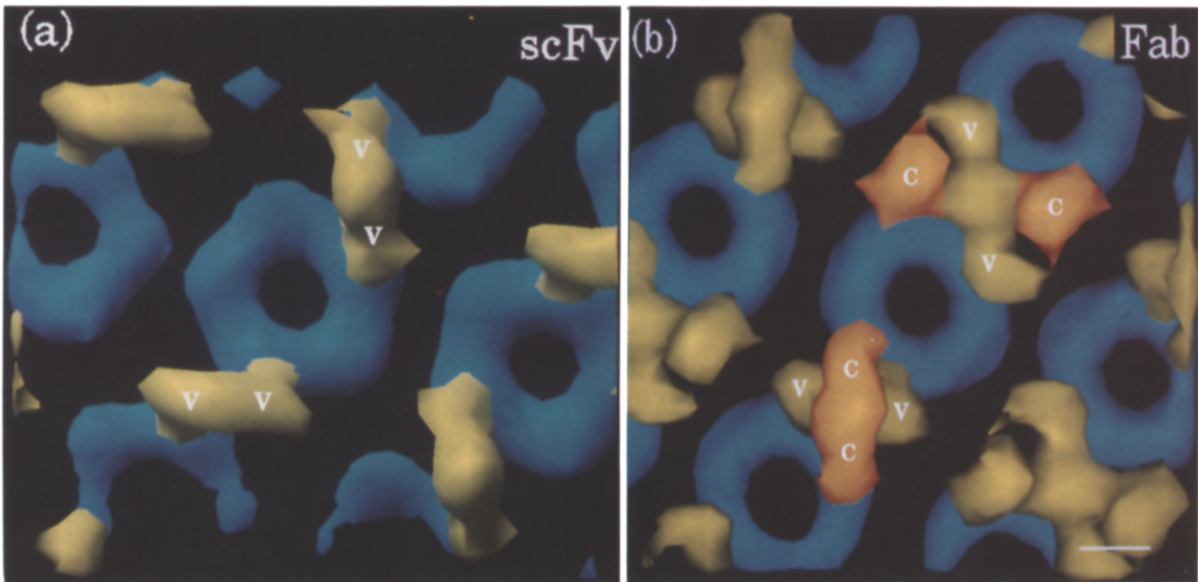


Figure 5. Synaptic View of Receptors Labeled with scFv35 and Fab35 Fragments
(a) scFv35; (b) Fab35.

The antibody fragments (gold) attach to sites that are separated by $\sim 144^\circ$ around the central axis of each receptor (blue). The Fab fragments show extra mass (stippled red) compared with the scFv fragments; this corresponds to the Fab fragment constant domains. Each antibody fragment mass seems to extend from one receptor to its neighbor, even though the fragments are monovalent. Therefore, each mass spanning neighboring subunits must contain two fragments that are not resolved from each other (V marks each variable domain and C marks each constant domain). The two different arrangements of antibody fragments arise because the receptors are grouped in pairs related by 2-fold axes. Bar, 50 Å.

The two antibody fragment masses connected to one receptor appear different from each other. In the case of the scFv35 fragments, this can be seen especially clearly in contour maps that represent their densities in sections parallel to the tube axis (Figure 6a). Although all the fragments are identical, they are connected to different α subunits of each receptor in nonequivalent positions in the

crystal lattice (which is composed of dimers of receptors) and, therefore, pair in different ways. To distinguish between the two antibody fragment masses, we identify the subunits they are bound to as α_δ (the α that touches the δ) and α_γ , based on the locations of the α and δ subunits determined previously (Kubalek et al., 1987; both α subunits are labeled in Figure 6).

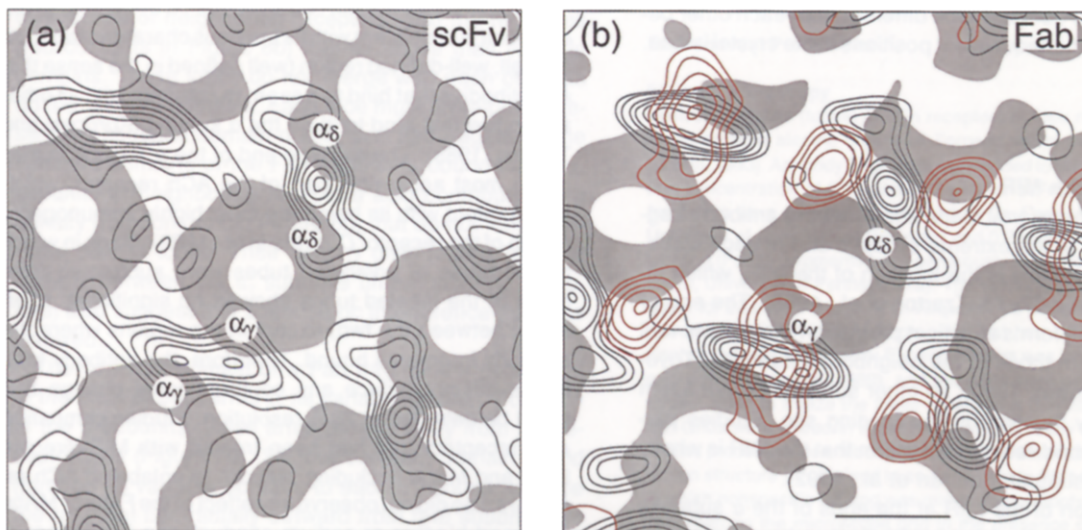


Figure 6. Sections through scFv35 and Fab35 Fragments, Overlying the Receptors to Which They Are Attached
(a) scFv35; (b) Fab35.

The antibody fragment variable domains (black contours) are located just above the receptors (shaded grey). The variable domains of the Fab fragments appear similar to the corresponding scFv fragments. The Fab fragments also have constant domains (red contours) above their variable domains. The assignments α_γ and α_δ are as in Kubalek et al. (1987). Bar, 50 Å.

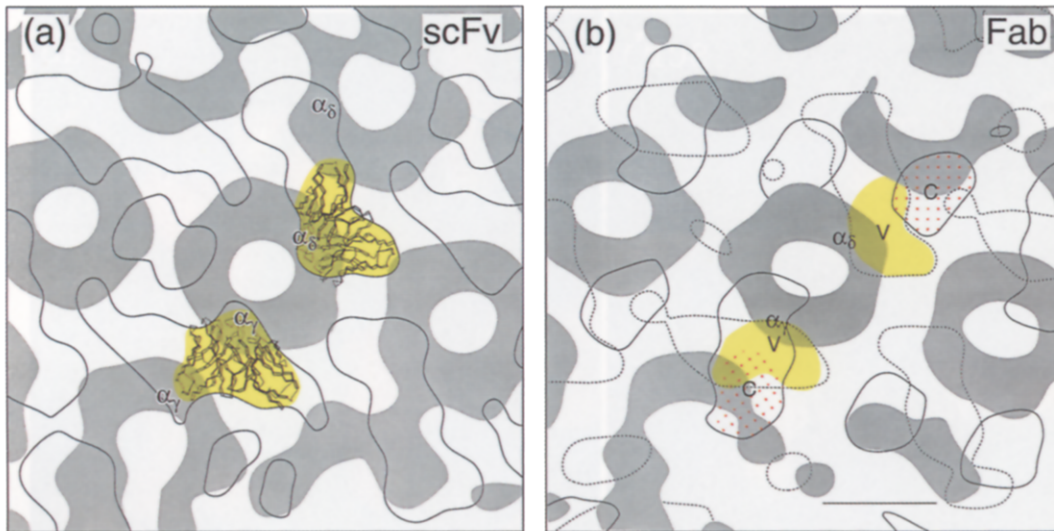


Figure 7. Inferred Locations and Orientations of Individual Antibody Fragments Relative to the Underlying Receptors

In (a), the atomic structure of the variable domain of a Fab fragment (taken from Lesk, 1991) was inserted into the outlines of the scFv35 fragments (taken from Figure 6a). The approximate space filled by each fragment is colored yellow. Although each of the outlines represents two fragments bound to neighboring receptors, the yellow fills more than half the space inside. This suggests that the binding of one scFv sterically inhibits the binding of its neighbor. Nevertheless, the outlines represent both fragments because they represent an average over the two alternative binding possibilities. In (b), the dashed lines outline the Fab35 variable domains, and the solid lines outline the constant domains (both taken from Figure 6b). Individual variable domains (marked as V) are colored yellow as in (a). Since the constant domain of a Fab fragment connects to the ends of both arms of its variable domain, the constant domain associated with each variable domain can be identified unambiguously (marked with red dots and as C). The variable domains project away from the central axis of the receptor, placing the two constant domains almost 100 Å apart. An Fc fragment cannot link constant domains this far apart, which explains why MAb35 cannot cross-link the two α subunits in one receptor. Bar, 50 Å.

The densities associated with the receptor-contacting domains of the Fab fragments (the black contours in Figure 6b) show similar features to those of the scFv fragments, identifying them unambiguously as the variable domains. The remaining densities in Figure 6b (red contours) must therefore correspond to the constant domains. The densities associated with the pairs of α_1 - and α_2 -bound Fab fragment constant domains look different from each other because of their nonequivalent positions in the crystal lattice.

Discussion

Location of the MIR

The three-dimensional maps show that the antibody fragments attach to the extreme synaptic end of each α subunit. Therefore, this is the location of the MIR, which includes residues 67–76 (Tzartos et al., 1988). The end of each α subunit forms a distinct protrusion that seems well separated from those of the neighboring subunits (Toyoshima and Unwin, 1990), so other subunits do not seem to be directly involved in the binding site. Studies performed on hybrid receptors confirm that the MIR is wholly within the α subunit (Loutrari et al., 1992).

This location of the MIR at the ends of the α subunits might be taken to be at odds with the results of a previous study (Kubalek et al., 1987), in which the antibody binding site appeared, in projection, to be near the interface between each α and its neighboring subunit. In fact, the three-dimensional densities composing the Fab35-labeled

receptor, when projected down the receptor axis, look like the densities in the previous study. The projection view can be misleading, however, because the top of the receptor, which includes the MIR, is twisted by about 36° around the channel axis (half the width of α subunit) (Toyoshima and Unwin, 1990) with respect to the main body of the structure.

The position of the MIR on a protrusion at the end of the α subunit is consistent with its previous characterization as a small, well-defined region (well defined in the sense that all antibodies that bind to it) on the α subunit (Kordossi and Tzartos, 1989). The extreme end of the α subunit is also in the most accessible part of the ACh receptor, which is consistent with its being the most highly immunogenic region of the receptor (Tzartos et al., 1982). Maps in which the densities of unlabeled tubes were subtracted from those of the labeled tubes showed no significant differences between the two, except in the regions where the antibody fragments bound. Therefore, the antibody fragments did not induce any conformational change that could be detected at 20 Å resolution. Studies comparing ACh receptors that had been treated with MIR-directed Fabs and MAbs (including MAb35) to unlabeled ACh receptors also did not observe any effect of the Fabs or MAbs on ligand binding or sodium conductance (Lindstrom et al., 1981; Wan and Lindstrom, 1985). Rather, MIR-directed antibodies induce myasthenia gravis by enhancing the degradation rates of postsynaptic ACh receptors (Drachman et al., 1978; Pumplin and Drachman, 1983).

Antibody Fragment Structures

Individual domains in the antibody fragments can be located by comparing the Fab35 and scFv35 structures. The antibody fragment densities in the scFv35 maps (the gold in Figure 5a and the black contours in Figure 6a) are composed only of the variable domains. Densities that closely correspond to these also appear in the Fab35 maps (the gold in Figure 4 and Figure 5b and the black contours in Figure 6b); hence the extra densities above the variable domains in the Fab35 maps must correspond to the constant domains (labeled red in Figure 4, Figure 5b, and Figure 6b).

To illustrate better the likely interaction of the antibody fragments with the ACh receptor, the X-ray structure of the variable domain of a Fab fragment was aligned by eye into the densities of the scFv35 map (Figure 7a). This structure consists of two antiparallel β -sheets (Lesk and Chothia, 1982), which appear as two arms that point away from the binding site. In the cases of both the α_s - and α_r -bound scFv35 fragments, one β -sheet extends more than half the distance toward the equivalent binding site of the neighboring receptor, indicating it would sterically interfere with the binding of an antibody fragment to that receptor. This suggests that at most only half of the MIR sites are occupied in the tubes, and that the antibody fragment "pairs" visualized are simply averages of the alternative occupancies. Indeed, the scFv fragments appear almost twice as dense in the "overlap" region (see Figure 6a), where there should always be density from one or other of the fragments, than they appear in regions where only one of the fragments would contribute density. Such observations of steric interference are unlikely to reflect the situation *in vivo*, in which the distribution of receptors is different.

Orientation of Fab35

The constant domains of the Fab fragments bound to the α_s subunits of neighboring receptors form the two lobes (red contours in Figure 6b) that lie above their variable domains. These lobes do not merge with each other as do the variable domains. Each lobe must therefore represent the constant domain of only one Fab fragment. The constant domains of the Fab fragments bound to the α_r subunits of neighboring receptors also contribute extra density (red contours in Figure 6b), but do not form obviously distinct lobes. Their density distributions (highest midway between the α_r subunits on neighboring receptors) also suggest that some steric interference might be involved.

The constant domain of a Fab fragment is connected to the ends of both arms of its variable domain. For each of the α subunits, these arms project away from the receptor axis (Figure 7a). So, the constant domain linked (through its variable domain) to each α subunit must be the one that lies radially outward from that subunit (see Figure 7b). Based on these assignments, the elbow angles (which relate the orientations of the variable and constant domains) of both Fab35 fragments are about 130° .

The constant domains of the two Fab fragments bound to a single receptor are almost 100 \AA apart. An Fc fragment

can only link Fab fragments that are about 50 \AA apart (Silverton et al., 1977). To attain this separation with the Fab fragments oriented as they are, their elbow angles would have to be close to 0° , which is well outside the observed range (130° – 180° ; Lesk and Chothia, 1988; Silverton et al., 1977). This explains why MAb35 cannot cross-link the two α subunits in one ACh receptor (Conti-Tronconi et al., 1981)—it binds in the wrong orientation.

If the Fab fragments of another antibody were to bind to the MIR in a different orientation so that their variable domains did not project almost directly away from the receptor axis, their constant domains could come within 50 \AA of each other. An Fc could link constant domains at this distance. MAbs to the MIR that bind to both α subunits on one receptor do exist (Conti-Tronconi et al., 1981).

ACh receptors in postsynaptic membranes are often closely packed (Fertuck and Salpeter, 1976; Heuser and Salpeter, 1979). Antibodies like MAb35, which project upward from the MIR and therefore do not have to snuggle in between receptors, could bind to them with a minimum of steric interference. Efficient binding of this kind may be particularly effective at enhancing the ACh receptor degradation rates responsible for the symptoms of myasthenia gravis.

Conclusion

The MIR, which contains residues $\alpha 67$ – 76 , is located at the extreme synaptic end of each α subunit of the ACh receptor. When bound to the MIR, the variable domains of MAb35 project almost directly away from the channel axis. This places the constant domains too far from the second MIR in the same receptor to allow cross-linking of the two α subunits by one MAb35 to occur. An antibody that binds to the MIR with a different orientation, however, could easily cross-link the two α subunits. MAb35 can bind to receptors with a minimum of steric interference because it projects away from the receptors into the synaptic cleft.

Experimental Procedures

Electron Microscopy

Vesicular crystals (tubes) of ACh receptors in their native lipids were prepared from electric organs of *Torpedo marmorata* as described (Unwin, 1993). Antibody fragments were added to the tube suspension at a concentration of 0.1 \mu g/ml (3.2 pM) for scFv35 labeling (scFv35 fragments were generously provided by Dr. Cara Marks, now at the University of California at Berkeley) and 0.2 mg/ml (4 nM) for Fab35 labeling (Fab35 fragments were generously provided by Dr. Jon Lindstrom, University of Pennsylvania). The suspensions were allowed to stand for 20 min to 3 hr at 4°C . Aliquots of 3 \mu l were then applied to the carbon side of holey carbon grids that had been recently glow-discharged with amylamine. Excess solution was blotted off from the grid side (Toyoshima, 1989), and the grids were plunged into liquid ethane slush to freeze the tubes rapidly in a thin film of amorphous ice. Grids were stored in liquid nitrogen until ready for use.

This procedure for antibody labeling gave essentially the same projection structure as obtained in an earlier study (Kubalek et al., 1987), in which nonspecific binding was minimized by applying Fab35 to the specimen on the microscope grid in the presence of cytochrome *c*. This earlier study also showed that Fab35 binds to the MIR sites on the tubes with high occupancy, whereas other nonMIR-directed Fab fragments do not bind to them significantly.

Grids were placed in a Philips EM420 microscope using Gatan cryo-holders and were kept below -160°C during microscopy. The microscope was equipped with a twin lens, a twin-bladed anticontaminator,

and a low dose kit. Coherent illumination was achieved by using a small second condenser aperture (50 μm diameter) and by strongly exciting the first condenser lens. A thin foil objective aperture, 50 μm in diameter, was always in place. The microscope was operated at 120 kV.

Thin, straight tubes that were suspended over holes in the carbon support film were imaged only if the ice appeared thick enough to make flattening unlikely, but thin enough to make the tubes easily visible. The search for such tubes was carried out in the defocused diffraction mode at a magnification of $\sim 1000\times$. Images were recorded at a magnification of 36,000 \times , on Kodak SO-163 film, at low ($<10\text{ e}^{-}/\text{\AA}^2$) doses. Specimen drift was minimized by adjusting the heater control on the cryoholder. The film was developed for 12 min in D19 developer.

Image Analysis

Images of tubes were selected according to the criteria of Toyoshima and Unwin, 1990. Fab35-labeled and scFv35-labeled tubes had to be of the (-15,5) and (-16,6) helical families, respectively. Micrographs were digitized with a Joyce-Loebl flatbed microdensitometer (extensively modified in-house) using a 10 μm effective spot size and 7.5 μm step size (corresponding to 2.15 \AA on the specimen). Image defocuses ranged from 1.2 to 1.8 μm .

Regions of each image that included exact multiples of the repeat distance of a tube were boxed off and Fourier transformed (DeRosier and Moore, 1970). The alignment of the tube axis with respect to the box, the correction for tilt of the tube away from the plane normal to the electron beam, and the extraction of layer lines from the Fourier transforms were done as described (Unwin, 1993), except that the rotation angle of the helix axis with respect to the box was refined to 0.01 $^\circ$ instead of 0.05 $^\circ$. The layer-line data from two to seven stretches along each tube were collected independently in this way. Only data extending to about 20 \AA resolution (within the first zero in the contrast transfer function) were used.

The tubes exhibit 2-fold symmetry about various radial axes because the repeating unit in the crystal lattice is a dimer of receptors. All the datasets from all the regions of Fab35-labeled tubes were brought to a common 2-fold phase origin and radial scale (the same origin and scale used in Toyoshima and Unwin, 1988); the same was done with all the datasets from the scFv35-labeled tubes (to the origin and scale used in Unwin, 1993). Layer lines from Fab35-labeled tubes were reassigned to obey the common helical selection rule $l = 3n + 67m$ ($n = 5n$); layer lines from scFv35-labeled tubes were reassigned to obey the rule $l = -81n + 253m$ ($n = 2n$) (Unwin, 1993). The different datasets were then averaged, weighting each dataset to maximize the 5-fold rotational symmetry (judged by eye) of the receptor within the membrane. Equatorial terms were averaged separately as in Unwin (1993). The features seen in maps of the averaged datasets were also seen in the maps of the individual datasets, but with more noise. The final maps were calculated by a Fourier-Bessel synthesis of the averaged datasets after data that was inconsistent with the 2-fold symmetry of the crystal had been filtered out. The appearance of the maps was not significantly altered by correcting for the contrast transfer function, so only the equators were corrected (assuming 7% amplitude contrast; Toyoshima and Unwin, 1988). Radial density distributions were determined by a Fourier-Bessel synthesis of only the equatorial data.

Control datasets were obtained from a similar analysis of three unlabeled (-15,5) and four unlabeled (-16,6) tubes (Toyoshima and Unwin, 1990; Unwin, 1993).

Surfaces of labeled receptors were rendered with AVS, using a threshold at which they would contain approximately 80%–100% of the volume of the receptor.

Acknowledgments

We thank Dr. Cara Marks for generously providing concentrated scFv35 stocks and Dr. Jon Lindstrom for providing concentrated Fab35 stocks. We also thank Drs. John Berriman, Nicola Konig, Jon Lindstrom, and Guido Zampighi for their advice and help. R. B. was supported by a Winston Churchill Scholarship, Glaxo Dorothy Hodgkin Scholarship, and Overseas Research Studentship. This research was supported, in part, by a grant (GM41449) from the National Institutes of Health.

The costs of publication of this article were defrayed in part by the payment of page charges. This article must therefore be hereby

marked "advertisement" in accordance with 18 USC Section 1734 solely to indicate this fact.

Received April 25, 1995; revised June 5, 1995.

References

- Barkas, T., Gabriel, J.-M., Mauron, A., Hughes, G. J., Roth, B., Alliod, C., Tzartos, S. J., and Ballivet, M. (1988). Monoclonal antibodies to the main immunogenic region of the nicotinic acetylcholine receptor bind to residues 61–76 of the α subunit. *J. Biol. Chem.* **263**, 5916–5920.
- Bellone, M., Tang, F., Millius, R., and Conti-Tronconi, B. M. (1989). The main immunogenic region of the nicotinic acetylcholine receptor: identification of amino acid residues interacting with different antibodies. *J. Immunol.* **143**, 3568–3579.
- Brisson, A., and Unwin, P. N. T. (1984). Tubular crystals of acetylcholine receptor. *J. Cell Biol.* **99**, 1202–1211.
- Brisson, A., and Unwin, P. N. T. (1985). Quaternary structure of the acetylcholine receptor. *Nature* **315**, 474–477.
- Chang, H. W., and Bock, E. (1977). Molecular forms of acetylcholine receptor: effects of calcium ions and a sulfhydryl reagent on the occurrence of oligomers. *Biochemistry* **16**, 4513–4520.
- Conti-Tronconi, B., Tzartos, S., and Lindstrom, J. (1981). Monoclonal antibodies as probes of acetylcholine receptor structure. II. Binding to native receptor. *Biochemistry* **20**, 2181–2191.
- Conti-Tronconi, B. M., McLane, K. E., Raftery, M. A., Grando, S. A., and Protti, M. P. (1994). The nicotinic acetylcholine receptor: structure and autoimmune pathology. *Crit. Rev. Biochem. Mol. Biol.* **29**, 69–123.
- DeRosier, D. J., and Moore, P. B. (1970). Reconstruction of three-dimensional images from electron micrographs of structures with helical symmetry. *J. Mol. Biol.* **52**, 355–369.
- Drachman, D. B., Angus, C. W., Adams, R. N., Michelson, J. D., and Hoffman, G. J. (1978). Myasthenic antibodies cross-link acetylcholine receptors to accelerate degradation. *N. Engl. J. Med.* **298**, 1116–1122.
- Fertuck, H. C., and Salpeter, M. M. (1976). Quantitation of junctional and extrajunctional acetylcholine receptors by electron microscope autoradiography after ^{125}I - α -bungarotoxin binding at mouse neuromuscular junctions. *J. Cell Biol.* **69**, 144–158.
- Heuser, J. E., and Salpeter, S. R. (1979). Organization of acetylcholine receptors in quick-frozen, deep-etched, and rotary-replicated *Torpedo* postsynaptic membrane. *J. Cell Biol.* **82**, 150–173.
- Kordossi, A. A., and Tzartos, S. J. (1989). Monoclonal antibodies against the main immunogenic region of the acetylcholine receptor: mapping on the intact molecule. *J. Neuroimmunol.* **23**, 35–40.
- Kubalek, E., Ralston, S., Lindstrom, J., and Unwin, N. (1987). Location of subunits within the acetylcholine receptor by electron image analysis of tubular crystals from *Torpedo marmorata*. *J. Cell Biol.* **105**, 9–18.
- LaRochelle, W. J., and Froehner, S. C. (1986). Determination of the tissue distributions and relative concentrations of the postsynaptic 43-kDa protein and the acetylcholine receptor in *Torpedo*. *J. Biol. Chem.* **261**, 5270–5274.
- Lesk, A. M. (1991). *Protein Architecture: A Practical Approach*. (Oxford: Oxford University Press).
- Lesk, A. M., and Chothia, C. (1982). Evolution of proteins formed by β -sheets. II. The core of the immunoglobulin domains. *J. Mol. Biol.* **160**, 325–342.
- Lesk, A. M., and Chothia, C. (1988). Elbow motion in the immunoglobulins involves a molecular ball-and-socket joint. *Nature* **335**, 188–190.
- Lindstrom, J., Tzartos, S., and Gullick, W. (1981). Structure and function of the acetylcholine receptor molecule studied using monoclonal antibodies. *Ann. NY Acad. Sci.* **377**, 1–19.
- Loutrari, H., Kokla, A., and Tzartos, S. J. (1992). Passive transfer of experimental myasthenia gravis via antigenic modulation of acetylcholine receptor. *Eur. J. Immunol.* **22**, 2449–2452.
- Loutrari, H., Tzartos, S. J., and Claudio, T. (1992). Use of *Torpedo*-mouse hybrid acetylcholine receptors reveals immunodominance of

- the α subunit in myasthenia gravis antisera. *Eur. J. Immunol.* **22**, 2949–2956.
- Marks, C. (1992). Antibody structure and function. Ph. D. thesis, University of Cambridge, Cambridge, England.
- Mitra, A. K., McCarthy, M. P., and Stroud, R. M. (1989). Three-dimensional structure of the nicotinic acetylcholine receptor and location of the major associated 43-kD cytoskeletal protein, determined at 22 Å by low dose electron microscopy and X-ray diffraction to 12.5 Å. *J. Cell Biol.* **109**, 755–774.
- Papadouli, I., Sakarellos, C., and Tzartos, S. J. (1993). High-resolution epitope mapping and fine antigenic characterization of the main immunogenic region of the acetylcholine receptor: improving the binding activity of synthetic analogues of the region. *Eur. J. Biochem.* **211**, 227–234.
- Protti, M. P., Manfredi, A. A., Horton, R. M., Bellone, M., and Conti-Tronconi, B. M. (1993). Myasthenia gravis: recognition of a human autoantigen at the molecular level. *Immunol. Today* **14**, 363–368.
- Pumplin, D. W., and Drachman, D. B. (1983). Myasthenic patients' IgG causes redistribution of acetylcholine receptors: freeze-fracture studies. *J. Neurosci.* **3**, 576–584.
- Saedi, M. S., Anand, R., Conroy, W. G., and Lindstrom, J. (1990). Determination of amino acids critical to the main immunogenic region of intact acetylcholine receptors by in vitro mutagenesis. *FEBS Lett.* **267**, 55–59.
- Sealock, R., Wray, B. E., and Froehner, S. C. (1984). Ultrastructural localization of the Mr 43,000 protein and the acetylcholine receptor in *Torpedo* postsynaptic membranes using monoclonal antibodies. *J. Cell Biol.* **98**, 2239–2244.
- Silverton, E. W., Navia, M. A., and Davies, D. R. (1977). Three-dimensional structure of an intact human immunoglobulin. *Proc. Natl. Acad. Sci. USA* **74**, 5140–5144.
- Toyoshima, C. (1989). On the use of holey grids in electron crystallography. *Ultramicroscopy* **30**, 439–444.
- Toyoshima, C., and Unwin, N. (1988). Contrast transfer for frozen-hydrated specimens: determination from pairs of defocused images. *Ultramicroscopy* **25**, 279–292.
- Toyoshima, C., and Unwin, N. (1988). Ion channel of acetylcholine receptor reconstructed from images of postsynaptic membranes. *Nature* **336**, 247–250.
- Toyoshima, C., and Unwin, N. (1990). Three-dimensional structure of the acetylcholine receptor by cryoelectron microscopy and helical image reconstruction. *J. Cell Biol.* **111**, 2623–2635.
- Tzartos, S. J., and Lindstrom, J. M. (1980). Monoclonal antibodies used to probe acetylcholine receptor structure: Localization of the main immunogenic region and detection of similarities between subunits. *Proc. Natl. Acad. Sci. USA* **77**, 755–759.
- Tzartos, S. J., Rand, D. E., Einarson, B. L., and Lindstrom, J. M. (1981). Mapping of surface structures of *Electrophorus* acetylcholine receptor using monoclonal antibodies. *J. Biol. Chem.* **256**, 8635–8645.
- Tzartos, S. J., Seybold, M. E., and Lindstrom, J. M. (1982). Specificities of antibodies to acetylcholine receptors in sera from myasthenia gravis patients measured by monoclonal antibodies. *Proc. Natl. Acad. Sci. USA* **79**, 188–192.
- Tzartos, S. J., Sophianos, D., and Efthimiadis, A. (1985). Role of the main immunogenic region of acetylcholine receptor in myasthenia gravis. An Fab monoclonal antibody protects against antigenic modulation by human sera. *J. Immunol.* **134**, 2343–2349.
- Tzartos, S., Hochschwender, S., Vasquez, P., and Lindstrom, J. (1987). Passive transfer of experimental autoimmune myasthenia gravis by monoclonal antibodies to the main immunogenic region of the acetylcholine receptor. *J. Neuroimmunol.* **15**, 185–194.
- Tzartos, S. J., Kokla, A., Walgrave, S. L., and Conti-Tronconi, B. M. (1988). Localization of the main immunogenic region of human muscle acetylcholine receptor to residues 67–76 of the α subunit. *Proc. Natl. Acad. Sci. USA* **85**, 2899–2903.
- Tzartos, S. J., Loutrari, H. V., Tang, F., Kokla, A., Walgrave, S. L., Milius, R. P., and Conti-Tronconi, B. M. (1990). Main immunogenic region of *Torpedo* electroplax and human muscle acetylcholine receptor: localization and microheterogeneity revealed by the use of synthetic peptides. *J. Neurochem.* **54**, 51–61.
- Unwin, P. N. T. (1993). Nicotinic acetylcholine receptor at 9 Å resolution. *J. Mol. Biol.* **229**, 1101–1124.
- Wan, K. K., and Lindstrom, J. M. (1985). Effects of monoclonal antibodies on the function of acetylcholine receptors purified from *Torpedo californica* and reconstituted into vesicles. *Biochemistry* **24**, 1212–1221.